Investigation of battery models and state of charge estimation for predictive energy management in hybrid electric aircraft

An Aloysius Wang*

September 20, 2022

Abstract

In the context of predictive energy management for hybrid electric aircraft, we investigate the effects of: (i) modelling the state-of-charge dependence of battery parameters, (ii) optimising cell configuration, and (iii) estimating the battery state-of-charge from noisy measurements.

1 Introduction

This report describes extensions of the model predictive control algorithm proposed by Doff-Sotta, Cannon & Bacic [1] for energy management of hybrid aircraft.

We first consider the model of the battery. Li-ion batteries exhibit complex transient behaviours and fluctuating battery parameters which are most accurately described using partial differential equations. However, from a control perspective, it is impractical to model the physics of the battery with unnecessarily high accuracy, and certain simplifications have to be made for the sake of computational efficiency. In the paper [1], the simplification made was to assume battery open-circuit voltage and internal resistance are constant. This results in a convex problem, which in turn guarantees the effectiveness and convergence of optimization algorithms (such as ADMM [1]). It is, however, important to check whether such a simple model captures enough of the physics to be used in a predictive control scheme.

We also explore how the proposed algorithm can be used to optimise design parameters such as the size of the battery array that should be carried by the aircraft. In particular, we focus on calculating optimal parameters for minimising CO_2 emissions per kg of payload while meeting design requirements.

Lastly, we propose practical methods to estimate battery state-of-charge and discuss how the control algorithm can be made robust against state estimation errors by adopting a scenario-based model predictive control approach.

2 An improved battery model

Experiments on Li-ion batteries (fig. 1) show that both open-circuit voltage (V_{oc}) and battery internal resistance (R_{internal}) vary with state-of-charge. We can incorporate this experimental data into the optimisation problem by assuming quadratic relationships between battery parameters and state-of-charge:

$$V_{\text{oc}} = \alpha_2 E^2 + \alpha_1 E + \alpha_0 \coloneqq u(E), \qquad R_{\text{internal}} = \beta_2 E^2 + \beta_2 E + \beta_0 \coloneqq r(E). \tag{1}$$

The parameters $\alpha_0, \alpha_1, \alpha_2$ and $\beta_0, \beta_1, \beta_2$ are obtained using least-squares polynomial regression. The dotted lines in fig. 1 show the lines of best-fit. We note here that the actual voltage and resistance used in computations have been scaled by an appropriate factor so as to match the application.

The motivation behind using a simple polynomial fit is to get an order-of-magnitude estimate of how much the predictive controller is affected by state of charge dependence of parameters while keeping the energy optimization problem tractable. If the optimum solution is not significantly affected by battery parameters, then there is no need to develop more sophisticated models.

*This report describes the results of work carried out July-September 2022 during a EUROP research project at the Department of Engineering Science, University of Oxford, UK.

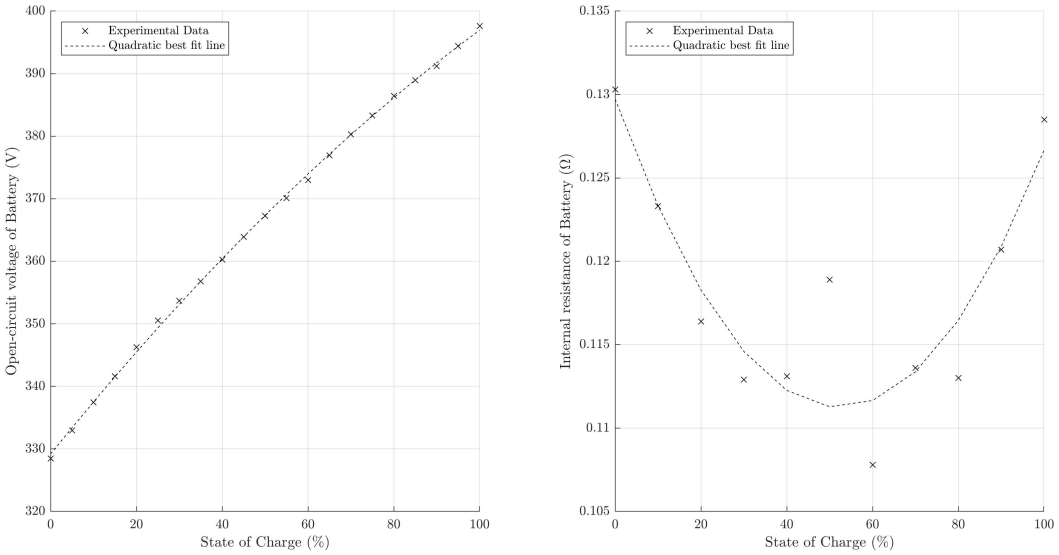

Figure 1: Experimental data of battery open-circuit voltage and internal resistance against battery state-of-charge. A quadratic least-squares approximation is used to model the SoC dependence.

With these assumptions, the open-loop optimisation problem proposed in [1] can be formulated as

$$\min_{\varphi,P_b,m,E,U,R} \sum_{i=0}^{n-1} \varphi_i \delta \qquad \text{subject to} \tag{2}$$

$$\begin{aligned}
\varphi_i &\geq f_{\varphi,i}(m_i, P_{b,i}, U_i, R_i),\\
m_i &= m(k\delta) - \sum_{l=0}^{i-1} \varphi_l \delta,\\
E_i &= E(k\delta) - \sum_{l=0}^{i-1} P_{b,l} \delta,\\
U_i &= u(E_i),\\
R_i &= r(E_i),\\
\underline{E} \leq E_i \leq \overline{E}, &\quad \underline{\varphi}_i \leq \varphi_i \leq \overline{\varphi}_i, \quad c(P_{b,i}, U_i, R_i) \leq 0
\end{aligned}$$

with

$$\begin{aligned}
f_{\varphi,i}(m_i, P_{b,i}, U_i, R_i) &= f_i(P_{\mathrm{drv},i}(m_i) - h_i^{-1}(\hat{g}(P_{b,i}, U_i, R_i)))\\
c(P_{b,i}, U_i, R_i) &= \max\left(h_i^{-1}(\hat{g}(P_{b,i}, U_i, R_i)) - \overline{P}_{em},\ P_{b,i} - \frac{U_i^2}{2R_i},\ \underline{P}_{em} - h_i^{-1}(\hat{g}(P_{b,i}, U_i, R_i))\right)\\
\hat{g}(P_{b,i}, U_i, R_i) &= \frac{P_{b,i}}{U_i}\left(U_i - \frac{P_{b,i}}{U_i} R_i\right),
\end{aligned}$$

Here U_i, R_i denote the open circuit voltage and internal resistance of the battery at the ith time-step, and the remaining variables and functions defined as in [1]. We note that by adopting a more accurate model of the battery, we are forced to give up the convexity of the problem. Henceforth we will refer to (2) as the nonconvex formulation of the optimisation. All numerical results are obtained from the open-source interior point optimiser IPOPT.

We discuss the validity of the convex model in the following two cases of interest.

1. The energy carried by batteries is much smaller than the total energy requirements of the whole flight ($\overline{E} \ll E_{\mathrm{tot}}$). From a practical perspective, current batteries are not nearly energy dense enough to compete with fuel, consequently, any realistic hybrid aircraft developed in the coming years would probably fall under this limit.

2. The energy carried by batteries is on the same order of magnitude as the total energy needed for the flight ($\overline{E} \sim E_{\text{tot}}$). From an environmental point of view, this is an important limit to consider as the ultimate goal would be for battery technology to replace fuel based combustion engines.

2.1 $\overline{E} \ll E_{\text{tot}}$

The parameters of the model used in simulations as shown in table 1 and are based on parameters of real Li-ion batteries detailed by Kokam [2]. We note that the total energy requirement for the flight is of the order 1.2×10^4 MJ, about 10 times the maximum battery capacity.

Model Parameters

Parameter	Value	Units
Battery open circuit voltage at full charge ($V_{\max}$)	800	V
Battery internal resistance at full charge ($R_{\max}$)	0.035	Ω
Upper limit of battery energy capacity ($\overline{E}$)	1487.5	MJ

Table 1

With these parameters, the optimum evolution of aircraft mass and battery state-of-charge is shown in fig. 2. The difference in total fuel burnt between the two formulations is 0.0834 kg, a fraction of the total fuel consumption (~ 1200 kg).

Intuitively, one may reason that if the battery contributes a small amount to the overall power, the change in its parameters over the flight would not significantly affect the optimal solution. However, if we vary $V_{\max}$ while keeping other model parameters constant, we see that there are values of $V_{\max}$ where the difference in fuel consumption between the convex and nonconvex formulations can be as large as 1 kg (fig. 3).

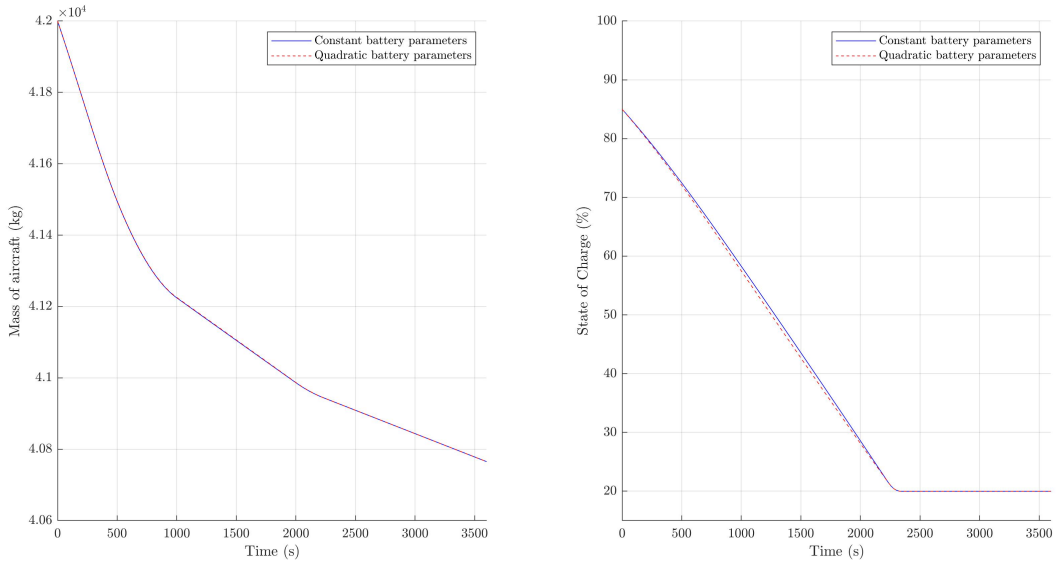

Figure 2: Evolution of mass and state-of-charge in the convex and nonconvex cases with model parameters detailed in Table 1.

To explain the trend seen in fig. 3, we consider the constraints that are active for different values of $V_{\max}$. In particular, we note that the maximum rate of power that can be drawn from the battery increases as a function of $V_{\text{oc}}^2/R_{\text{internal}}$. This means that when $V_{\max}$ is small, the battery will be limited by its rate of discharge. Since the objective of the optimisation is to reduce fuel consumption, if the rate maximum of discharge is small enough such that battery can discharge at maximum capacity for the entire flight, then that would clearly be the optimum strategy. In fig. 4, we see exactly that. When $V_{\max}$ is 90 V, throughout the duration of the flight where power demand is positive, the battery discharges at its upper limit (as indicated by the dashed lines). A quick calculation shows that the value of $v(E)^2/r(E)$ is greater than 1 when the state-of-charge

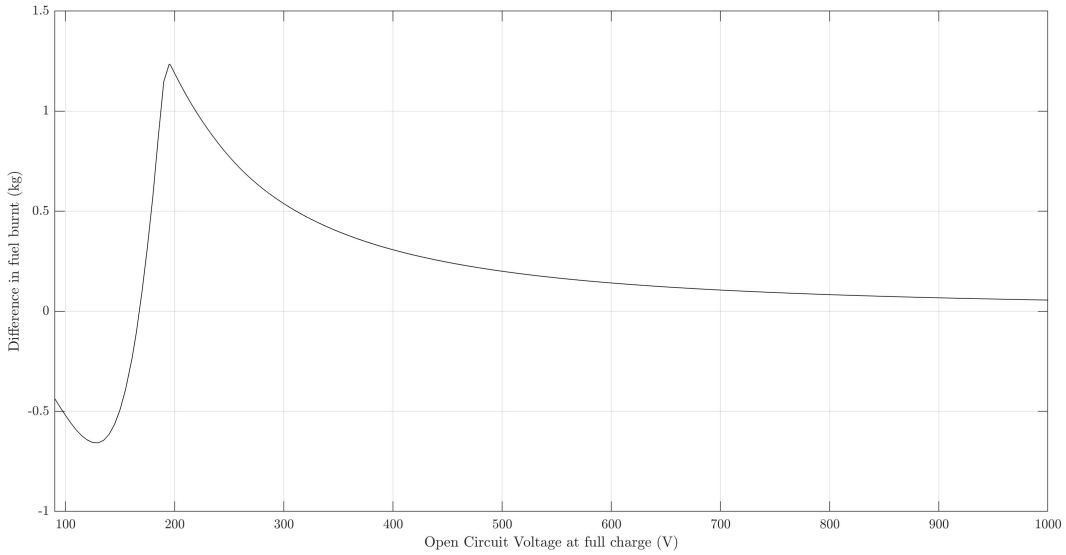

Figure 3: Graph of fuel consumed in the nonconvex formulation - fuel consumed in convex formulation.

$E/\overline{E} > 0.539$, so in this limit where $V_{\max}$ is small, the battery in the nonconvex formulation will discharge at a faster rate than the in the convex formulation, and less fuel will be burnt overall.

On the other extreme, when $V_{\max}$ is large, the constraint that is dominant will be the capacity of the battery $\overline{E}$. From fig. 4, when $V_{\max}$ is 800 V, the optimal operating point is seen to be far below the physical maximum rate of discharge. In this case, since the critical constraints in both formulations are the same, we get similar solutions. Therefore, the accuracy lost from using a convex formulation is negligible.

When $V_{\max}$ lies between these two extremes, both constraints will influence the solution, and it is not obvious how large the discrepancy between the two formulations will be.

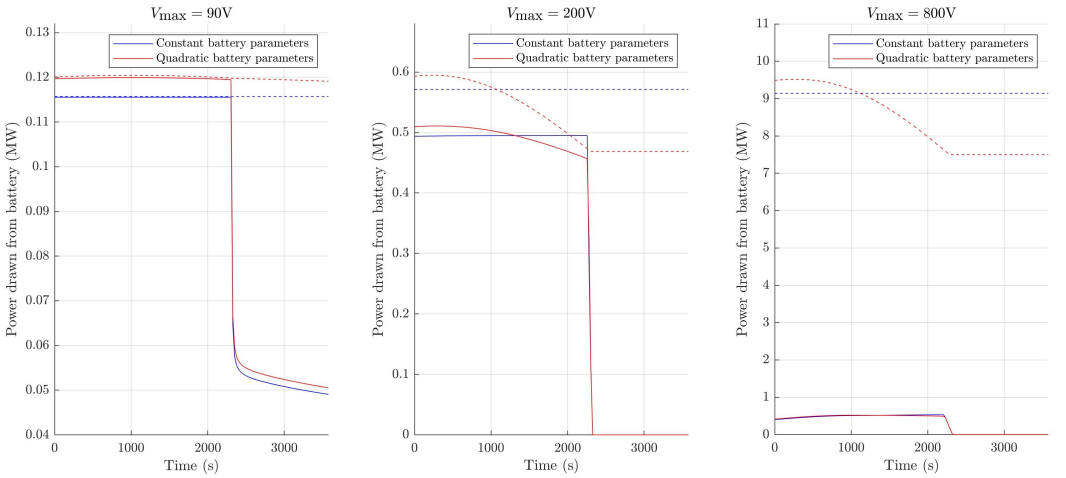

Figure 4: Evolution of battery rate of discharge P_b for different values of $V_{\max}$, where the dashed lines represent the maximum rate of discharge.

From a practical perspective, if the level of hybridisation for the aircraft is low, we would most likely be in the limit where $\overline{E}$ is the dominant constraint. In such a situation, adopting a convex formulation would not significantly change the optimal solution. However, if the level of hybridisation of the aircraft is high, the simulation results above suggest that a more sophisticated battery model may lead to significant fuel savings.

2.2 $\overline{E} \sim E_{\text{tot}}$

In the following simulations, $\overline{E}$ was set to 10200 MJ. As before, we vary $V_{\max}$ and plot the difference between the convex formulations and nonconvex formulations (fig. 5).

The graph obtained when $\overline{E} \sim E_{\text{tot}}$ has the same overall shape as when $\overline{E} \ll E_{\text{tot}}$. However, a key difference is the magnitude of discrepancies between the two formulations is much larger when $\overline{E} \sim E_{\text{tot}}$. Compounded with the fact that the total amount of fuel consumed decreases when $\overline{E}$ increases, by proportion of total fuel burnt, the maximum error of the convex formulation can be fairly significant in the $\overline{E} \sim E_{\text{tot}}$ limit. This highlights the unsurprising importance of an accurate battery model for highly hybridised aircraft.

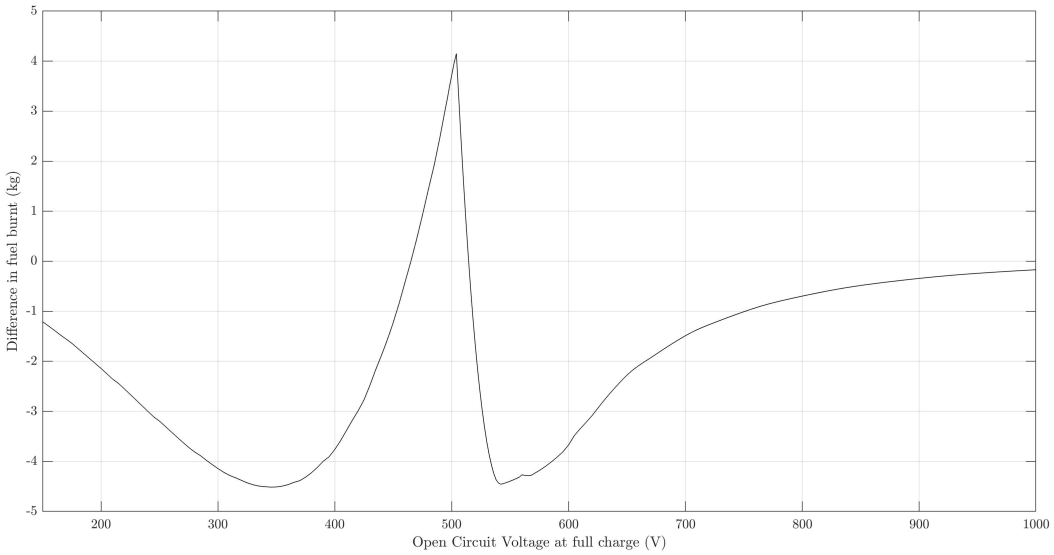

Figure 5: Graph of fuel consumed in the nonconvex formulation - fuel consumed in convex formulation in the $\overline{E} \sim E_{\text{tot}}$ limit.

2.3 Discussion of results

At the operating point of interest, our simulations show that the discrepancy between the two formulations proposed is insignificant, which suggests that the convex model can be safely used without sacrificing accuracy. However, the results above also highlight two possible scenarios where the convex model may fail to give the optimum solution: (1) when operation is limited by rate of discharge and (2) when the degree of hybridisation is high.

3 Optimising $\overline{E}$

In this section, we discuss practical considerations on the number of batteries that should be carried for the proposed flight path.

When we increase the number of batteries carried by the aircraft, the total power required of the gas turbine will fall, and hence total fuel consumption decreases. However, this does not come without cost. The trade-off made is that the batteries themselves will have some weight and this lowers the amount of payload that the aircraft can carry. We therefore seek to investigate if there is an arrangement of batteries such that the fuel savings due to the batteries is large enough to compensate for their weight.

In order to get the desired maximum current for application, we require maximum bus voltage to be 800 V. To meet this requirement, we consider m parallel lines of n batteries in series (fig. 6) such that the maximum voltage across the $n \times m$ array is as close to 800 V as possible. Using battery data from Kokam [2], we do a grid-search across a variety of different battery models and different values of m, with the objective of maximising the payload weight $m_{\text{payload}} = \text{Maximum take-off weight} - m_{\text{fuel}} - m_{\text{bat}}$. The results are shown in fig. 7.

It is clear from fig. 7 that the amount of fuel saved by increasing the number of batteries is not sufficient to compensate for their weight. However, the payload weight is one of many objectives

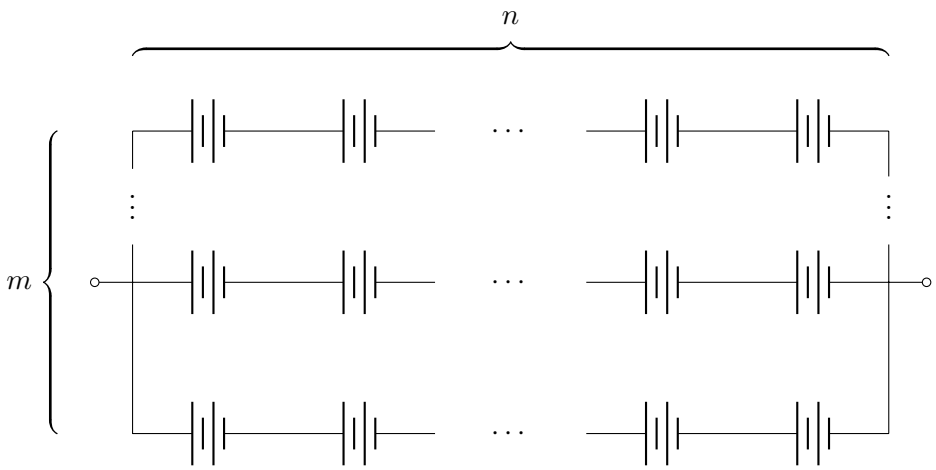

Figure 6: Schematic for battery array

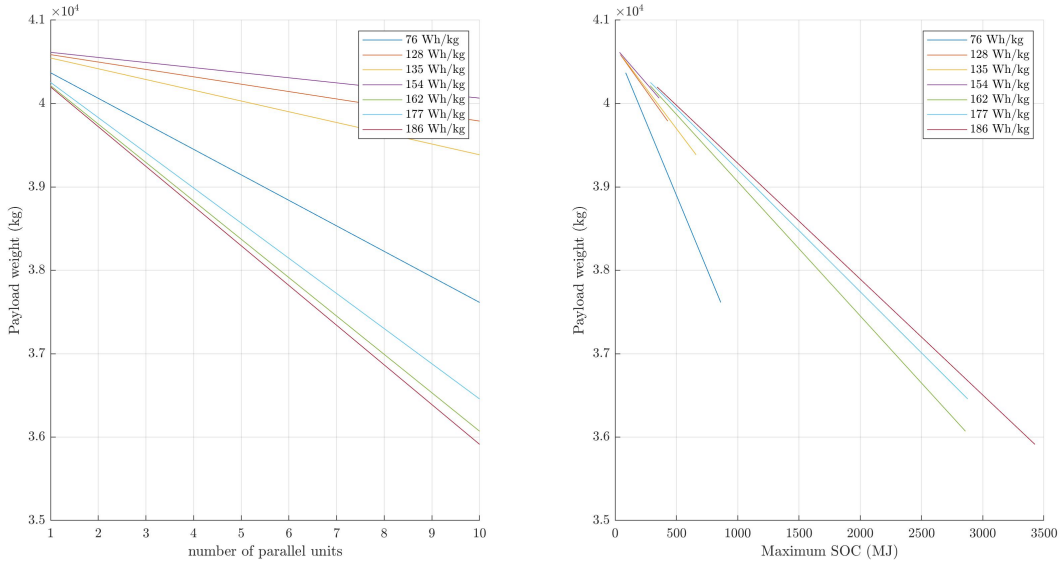

Figure 7: Maximum payload weight for different battery arrangements

that we can consider. Since the purpose of using batteries is to reduce carbon emissions, a more suitable objective may be the CO_2 emissions per kg of payload. If we assume that the amount of CO_2 produced is proportional to the mass of fuel burnt, we can equivalently minimise the fuel burnt per kg of payload. The results of the grid search with this new objective is shown in fig. 8.

From fig. 8, we see that if the batteries are sufficiently energy dense, we can reduce the CO_2 emissions per kg of payload. The model parameters of the optimum configuration are as shown in table 2. With these parameters, the difference between fuel burnt in the convex and nonconvex formulation is 0.104 kg. This difference corresponds to 0.013% of total fuel burnt and is therefore negligible.

Model Parameters

Parameter	Value	Units
Battery open circuit voltage at full charge ($V_{\max}$)	796.47	V
Battery internal resistance at full charge ($R_{\max}$)	7.167	mΩ
Upper limit of battery energy capacity ($\overline{E}$)	10322	MJ

Table 2

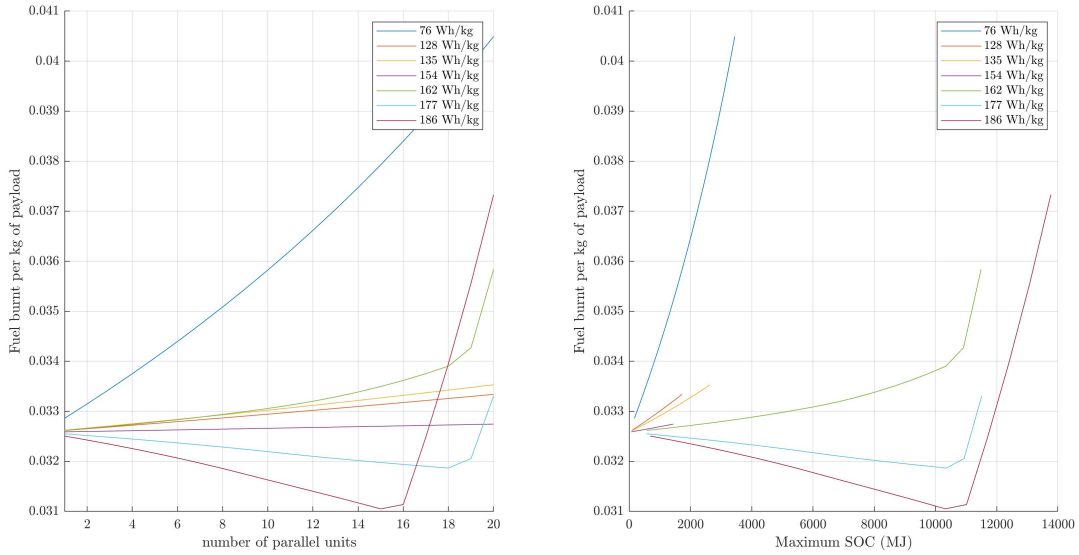

Figure 8: Fuel burnt per kg of payload for different battery arrangements

4 Robustness to errors in state-of-charge estimation

In the previous sections, we tacitly assumed that the state-of-charge E is known exactly. The reality is that state-of-charge cannot be measured directly, and must therefore be estimated in a suitable fashion. In this section, we investigate the use of a Kalman filter for state-of-charge estimation and discuss how we can make the predictive energy management algorithm more robust to uncertainties in state-of-charge estimates by incorporating Kalman filters into the control algorithm.

We introduce the following discrete state-space system to model battery dynamics:

$$\mathrm{SOC}_{k+1} = \mathrm{SOC}_k - \frac{\Delta t}{E_{\max}} \frac{U_k}{2R_k} \left(U_k - \sqrt{U_k^2 - 4R_k P_{c,k}} \right) + w_k, \tag{3}$$

$$I_k = \frac{1}{2R_k} \left(U_k - \sqrt{U_k^2 - 4R_k P_{c,k}} \right) + \epsilon_k^I, \tag{4}$$

$$V_k = \frac{2R_k P_{c,k}}{U_k - \sqrt{U_k^2 - 4R_k P_{c,k}}} + \epsilon_k^V. \tag{5}$$

Here, we treat power required by the electrical motor $P_{c,k}$ as the control input, the state-of-charge SOC_k as an internal state, and the output current I_k and terminal voltage V_k as outputs of the system that are provided by noisy sensor measurements. R_k and U_k are the internal resistance and open-circuit voltage of the battery respectively, and we assume they follow the relationship in (1). Lastly, w_k represents process noise and ϵ_k^I, ϵ_k^V represent measurement noise. These noise sources are assumed to be zero-mean and independent with variances σ_w^2, σ_I^2 and σ_V^2 respectively. In canonical form, (3)-(5) can be written as

$$\mathrm{SOC}_{k+1} = f(\mathrm{SOC}_k, P_{c,k}) + w_k \tag{6}$$

$$\begin{pmatrix} I_k \\ V_k \end{pmatrix} = h(SOC_k, P_{c,k}) + \begin{pmatrix} \epsilon_k^I \\ \epsilon_k^V \end{pmatrix}. \tag{7}$$

We propose three different methods of filtering for state-of-charge estimation. In increasing order of sophistication, they include a linearised Kalman filter (where the equations of state are linearised about the solution obtained from (2)), an extended Kalman filter and an unscented Kalman filter [3]. Fig. 9 (left) shows the state-of-charge estimates obtained from the different Kalman filters for a single realisation of the noise sequences. The right-hand plot shows how the average ℓ_2 norm of estimation over the duration of the flight varies with σ_w^2. From fig. 9, we see that at low noise power, the linearised Kalman filter has the worst performance, but this discrepancy drops off as process noise increases. We also note that the unscented Kalman filter provides no clear improvement despite its increased sophistication. We therefore chose to adopt an extended Kalman filter for our application.

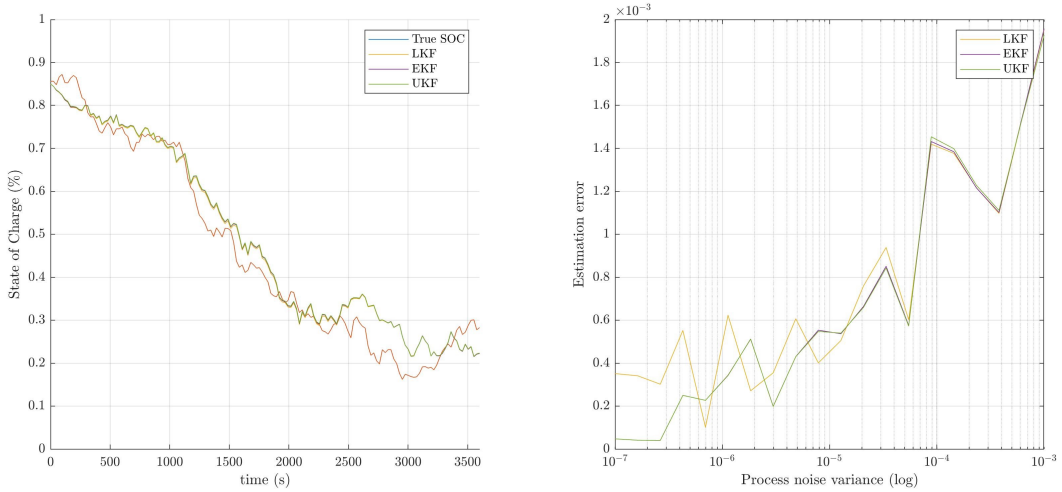

Figure 9: Left - An example of state-of-charge estimates with $\sigma_w^2 = 2e-4$, and $\sigma_I^2 = 5000, \sigma_V^2 = 1000$. Right - The average ℓ_2 norm of estimation error over 100 realisations of noise sequences at different process noise variance.

4.1 Sensitivity of optimisation to noise

We now propose a method of investigating the sensitivity of the optimisation to process noise. This is addressed by estimating the worst-case effect of state estimation errors on the open-loop energy management optimisation problem.

For a problem consisting of N time-steps, we create a receding horizon solution as follows. We first generate K samples of the N-step process noise and measurement noise sequences, denoted $w_{k,n}$, $\epsilon^I_{k,n}$, $\epsilon^V_{k,n}$, for $1 \leq k \leq K$ and $1 \leq n \leq N$, where K is a suitably large number. At each time step n, we use these noise samples to generate K samples of the current charge estimate using K instances of an extended Kalman filter, denoted $\hat{E}_{k,n}$, for $1 \leq k \leq K$ and $1 \leq n \leq N$. We compute at each time-step the worst-case optimal predicted energy usage based on the estimates $\hat{E}_{k,n}$, for $1 \leq k \leq K$ and use this to determine the current control variable. This process is summarised as follows.

Initialisation: Set an initial state of charge estimate $\hat{E}_0 = \mathbb{E}[E_0]$ and solve optimisation problem (2) with $E(k\delta) = \hat{E}_0$ to get the optimum $P_{c,0}$.

At each time-step $\mathbf{n = 1, 2, \ldots, N}$:

1. For each $k = 1, 2, \ldots, K$, generate an state-of-charge estimate $\hat{E}_{k,n}$ using an extended Kalman filter.
2. Solve the following optimisation problem to get the optimum $P_{c,n}$.

$$\min_{\varphi, m, P_{b,1}, \ldots, P_{b,K}, E_1, \ldots, E_K, U_1, \ldots, U_K, R_1, \ldots, R_K} \sum_{i=0}^{N-n} \varphi_i \delta \qquad \text{subject to} \tag{8}$$

$$\varphi_i \geq \max\left(f_{\varphi,i}(m_i, P_{b,1,i}, U_{1,i}, R_{1,i}), \ \ldots, f_{\varphi,i}(m_i, P_{b,K,i}, U_{K,i}, R_{K,i})\right),$$

$$m_i = m(n\delta) - \sum_{l=0}^{i-1} \varphi_l \delta,$$

$$E_{1,i} = \hat{E}_{1,n} - \sum_{l=0}^{i-1} P_{b,1,l}\delta, \ \ \ldots, E_{K,i} = \hat{E}_{K,n} - \sum_{l=0}^{i-1} P_{b,K,l}\delta,$$

$$U_{1,i} = u(E_{1,i}), \ \ \ldots, U_{K,i} = u(E_{K,i}),$$

$$R_{1,i} = r(E_{1,i}), \ \ \ldots, R_{K,i} = r(E_{K,i}),$$

$$\underline{\varphi}_i \leq \varphi_i \leq \overline{\varphi}_i, \quad \underline{E} \leq E_{1,i}, \ldots, E_{K,i} \leq \overline{E},$$
$$c(P_{b,1,i}, U_{k,i}, R_{k,i}), \ldots, c(P_{b,K,i}, U_{k,i}, R_{k,i}) \leq 0,$$

where all relevant variables and functions are defined as in (2).

Intuitively, in (8) we calculate a value of $P_{c,n}$ that would allow for constraints to be met in the worse case scenario - this therefore gives us an estimate of an upper bound on the amount of fuel that needs to be burnt. Fig. 10 shows the simulation results for this optimisation, where all tests were run with $K = 20$, $\sigma_w^2 = 5e-5$, $\sigma_I^2 = 5000$ and $\sigma_V^2 = 1000$. Constraint violations were handled by setting the lower limit on state of charge equal to the current state of charge whenever this falls below the bound $\underline{E}$. Table 3. summarises the simulation results at different process noise variance. It is unsurprising that the nosier the system is, the more conservative the solution is in its usage of the battery. We also note here that the proposed formulation would not be feasible as a method of constructing a real-time controller as the time for computation is prohibitively high, with $K = 20$, $N = 150$ taking about 100 minutes to run using IPOPT to solve the nonconvex optimization (8).

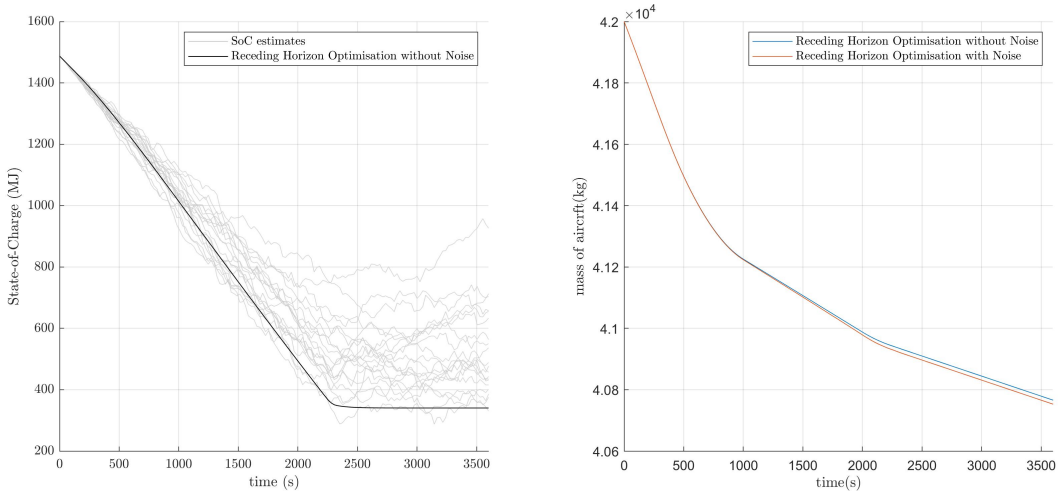

Figure 10: Left - State-of-charge estimates across 20 trials with $\sigma_w^2 = 5e-5$, and $\sigma_I^2 = 5000, \sigma_V^2 = 1000$. Right - Evolution of aircraft mass for a receding horizon optimisation with and without noise.

Results of Receding Horizon optimisation

Process Noise Variance σ_k^2	Difference in mass of fuel burnt (kg)
2e-4	32.26
1e-4	22.13
5e-5	13.12
1e-5	5.24

Table 3

4.2 A potential model predictive controller with SoC estimation

In this section we describe a possible method for incorporating state-of-charge estimation into a model predictive controller for the energy management problem. This uses a scenario optimisation approach, in which, at each time step, a set of K samples is drawn from the probability distribution of the current state of charge estimate provided by a single extended Kalman Filter. Following which, K samples of the future process noise sequence in (3) are generated and these samples are then used to optimise the empirical mean of predicted performance subject to constraints being satisfied by all samples. This is summarised as follows.

Initialisation: Set an initial state of charge estimate $\hat{E}_0 = \mathbb{E}[E_0]$.

At each time-step $\mathbf{n = 0, 1, \ldots, N-1}$:

1. If $n \geq 1$, compute $\hat{E}_n$ using an extend Kalman filter.
2. Generate K scenarios for the current state-of-charge, $\tilde{E}_n^1, \ldots, \tilde{E}_n^K$ by sampling the distribution $\mathcal{N}(\hat{E}_n, \hat{P}_n)$ and K scenarios for future process noise, $\tilde{w}_k = \{\tilde{w}_{k,0}, \ldots \tilde{w}_{k,N-n+1}\}$, $k = 1, \ldots, K$.
3. Solve the following optimisation problem

$$\min_{\varphi_1, \ldots, \varphi_K, m_1, \ldots, m_K, P_{b,1}, \ldots, P_{b,K}, E_1, \ldots, E_K, U_1, \ldots, U_K, R_1, \ldots, R_K} \frac{1}{K} \sum_{k=1}^{K} \sum_{i=0}^{N-n} \varphi_i \delta \qquad \text{subject to} \qquad (9)$$

$$\begin{aligned}
\varphi_{k,i} &\geq f_{\varphi,i}(m_{k,i}, P_{b,k,i}, U_{k,i}, R_{k,i}) \\
m_{k,i} &= m(n\delta) - \sum_{l=0}^{i-1} \varphi_{k,l} \delta, \\
E_{k,i} &= \tilde{E}_n^k - \sum_{l=0}^{i-1} P_{b,k,l} \delta + \sum_{l=0}^{i-1} \tilde{w}_{k,l}, \\
U_{k,i} &= u(E_{k,i}), \\
R_{k,i} &= r(E_{k,i}), \\
\underline{\varphi}_{k,i} \leq \varphi_{k,i} &\leq \overline{\varphi}_{k,i}, \quad \underline{E} \leq E_{k,i} \leq \overline{E}, \\
c(P_{b,k,i}, U_{k,i}, R_{k,i}) &\leq 0, \quad P_{b,1,0} = \cdots = P_{b,K,0}.
\end{aligned}$$

4. Compute the control variable $P_{c,n}$ by using the optimal solution for $P_{b,1,0}$

$$P_{c,n} = P_{b,1,0} - P_{b,1,0}^2 \frac{r(\hat{E}_n)}{u(\hat{E}_n)^2}. \qquad (10)$$

The evolution of the battery state of charge using the proposed controller is shown in fig. 11. The optimisation was run 30 times with the parameters $N = 60$, $K = 20$, $\sigma_w^2 = 2e-5$, and $\sigma_I^2 = 5000, \sigma_V^2 = 1000$. Each grey line in fig. 11 illustrates an individual simulation. Across the 30 individual trials, the range of fuel burnt varies between 1225.9 kg and 1241.2 kg. Violations of state of charge constraints were handled by setting the lower limit on state of charge equal to the current state of charge whenever this falls below the lower constraint $\underline{E}$.

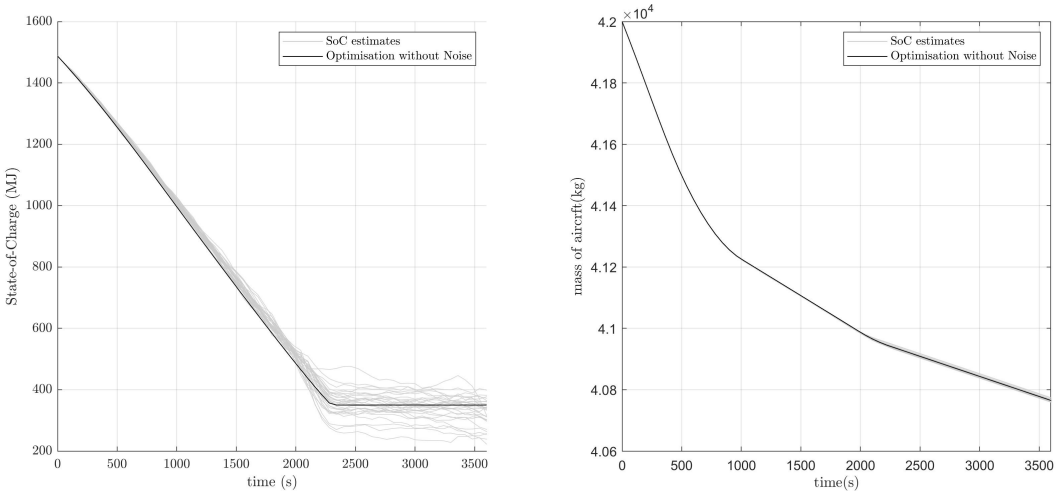

Figure 11: Left - evolution of state across 30 trials. Right - evolution of aircraft mass for each trial.

In contrast to the sensitivity evaluation in Section 4.2, the approach described in this section uses a single EKF and thus requires a single pair of measurements I_n, V_n at each time-step n. Uncertainty in the state estimate is represented by samples of the distribution of the EKF estimation error, and uncertainty in the future predicted battery state-of-charge is represented by samples of the future process noise sequences.

Therefore in principle this approach provides a predictive control scheme that is implementable. However, the battery parameters are assumed to depend on the state of charge here, so problem (9) is nonconvex and was solved using IPOPT, resulting in computation times of order 100 s at each sampling instant, which may not be suitable for real-time implementation. On the other hand, although the EKF necessarily employs the battery model (3)-(5), the online optimization (9) could be performed assuming constant battery parameters, provided the operating conditions are such that the effects of this simplification on performance are negligible, as described in Section 2. This would replace (9) with a convex optimization problem that would be more suitable for computing a predictive control law in real-time.

Using theoretical results from scenario optimization and statistical learning it would be possible to determine bounds on the probability that constraints will be violated as a function of the number of samples K. This is left as future work.

5 Conclusions

In this report, we have investigated the effects of simplifying assumptions in the battery model employed in the paper by Doff-Sotta, Cannon, & Bacic [1]. We identified two situations in which a more accurate battery model may be beneficial, namely when operation is limited by rate of discharge and when the degree of hybridisation is high. We also acknowledge here that the battery model used in our investigations ignores the transient behaviour observed in Li-ion batteries. This omission is not completely unjustified. The transient behaviour of Li-ion batteries is only dominant when there are large fluctuations in the rate of discharge, which are highly unlikely to occur in the solutions that we obtain. Nonetheless, this may be an interesting point of investigation.

We have also shown that it is possible to reduce the CO_2 emissions per kg of payload through a suitable choice of battery cell configuration. This result validates current work on developing hybrid aircraft in order to reduce the carbon footprint of the aviation industry.

Lastly, we proposed a method of incorporating state-of-charge estimation into a scenario model-predictive controller. We recommend the use of an extended Kalman filter and propose a scenario MPC algorithm to account for estimation errors. We provide simulation results showing the potential performance of this approach. As a future research direction these simulations could be used to check the accuracy of theoretical bounds on performance and constraint violations derived from scenario optimisation theory.

References

[1] Doff-Sotta, M., Cannon, M., & Bacic, M. (2022). Predictive Energy Management for Hybrid Electric Aircraft Propulsion Systems. IEEE Transactions on Control Systems Technology (early access). https://doi.org/10.1109/tcst.2022.3193295

[2] [ht] Kokam. (n.d.). KOKAM Li-ion/Polymer Cell. Retrieved September 8, 2022, from https://www.west-l.com/uploads/tdpdf/sf_kokam_cell_brochure_v.1.pdf

[3] He, W., Williard, N., Chen, C., & Pecht, M. (2013). State of charge estimation for electric vehicle batteries using unscented Kalman filtering. Microelectronics Reliability, 53(6), 840–847. https://doi.org/10.1016/j.microrel.2012.11.010